Polymer dispersed liquid crystals and related electro-optical devices - An overview

Amelia Carolina Sparavigna

Polymer dispersed liquid crystals and related electro-optical devices
An overview

Amelia Carolina Sparavigna[1]

1 – Department of Applied Science and Technology, Politecnico di Torino, Torino, Italy

ORCID ID 0000-0003-4502-8974

Keywords: Liquid crystals, PDLCs, Displays, Digital papers, Light shutters, Holographic displays, H-PDLCs.

ABSTRACT. To have a polymer dispersed liquid crystal (PDLC), the liquid crystalline material is dispersed into a liquid polymer. When the polymer changes from liquid to solid, the liquid crystal becomes incompatible with the polymer and creates dispersed droplets throughout the polymeric film. The film can be processed by standard techniques to have large and environmentally robust displays and light shutters. This paper describes PDLC films and their properties in a simplified approach, suitable for teaching the devices based on such films to students of university courses.

1. Introduction

In a discussion about the first pioneering works on liquid crystals [1,2], we have seen that liquid crystals dispersed in polymers began being studied in the early 1980s [3-5]. Therefore, these materials – known as PDLCs, Polymer Dispersed Liquid Crystals - are used in applications from several years, and today can be considered as materials for a mature technology. For this reason, it is convenient to discuss them in detail to show the development of the related technological area.

There are several manners of preparing blends of liquid crystals (LC) and polymers, which can lead to different types of materials, including polymer dispersed liquid crystals, polymer networks filled with liquid crystals, polymer/LC/dyes systems, and many others. In them, the polymers have the relevant role of achieving the desired effects from the presence of liquid crystals. The most important features that the polymeric component must have, besides the ability to form an amorphous film, are high transparency, inertness in relation to a liquid crystal and a good miscibility with mesogens in the liquid state. When the polymers are used in the stabilization of the droplets of the liquid crystal, we have PDLC materials.

Here, we propose an overview concerning the PDLC materials and their related properties. We will discuss the film response to an electric field, evaluating the threshold field and the role of anchoring of the nematic material to the surface of the droplets. We will use a simplified approach, suitable for teaching the devices based on such films to students of engineering courses. After the theoretical discussion, we will describe some devices and applications.

2. PDLC

The researches on PDLCs and the potentialities of their use in a variety of electro-optical applications including switchable windows, displays and other devices have been discussed in several references [6-12]. The core of the devices is made of a 10–25 μm thick film of PDLC material between transparent conducting electrodes. PDLC films consist of nematic micron-sized droplets dispersed in a polymer matrix. The optical response is based on the electrically controlled light scattering by droplets. An applied electric field aligns the nematic in the droplets to yield a non-scattering or transparent state. Surface interactions at the droplet wall or a non spherical droplet shape return the droplets to the original orientation in the absence of the field, giving a scattering or opaque state. A competition between the applied field, and the elastic and viscous torques of the liquid crystal governs the response times and switching voltages of such devices.

The operating mode is the following. Nematic droplets are randomly oriented in the opaque state and the film has a translucent white appearance due to light scattering properties of the droplets. Upon application of a field the droplets align in a direction parallel to the field. If the refractive index of nematic approximately matches the refractive index of the polymer matrix, the film will switch to a transparent state. Upon removal of the field, the droplets return to their original random orientation and the film returns to its opaque state.

3. The threshold electric field

Some experimental investigations [13-15] displayed that the liquid crystal droplets suspended in isotropic matrices exhibit a radial or a bipolar configuration, according to the anchoring conditions at the droplet surface, when the external electric field E is zero (see the Figure 1). However, above a threshold value of the electric field, the radial configuration becomes axial, and in the case of a bipolar droplet, the bipolar axis turns parallel to the electric field. It means then the droplet can be driven by field E.

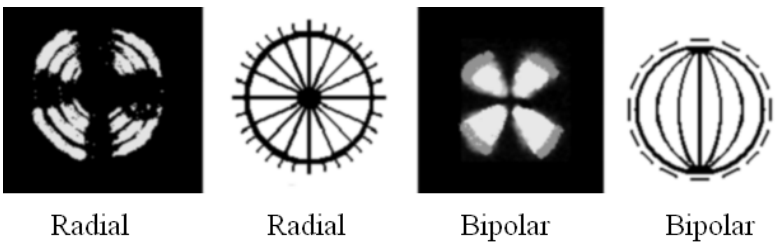

Figure 1 - Radial and bipolar direction of the director field and the corresponding textures that we can observe in polarized light microscopy with crossed polarisers. Note the different anchoring conditions at the surface of the droplets.

Several physical effects were observed as shown in [12,14]. In the Reference 13, the threshold field was measured for 5CB in a silicone elastomer and the role of droplet diameter investigated. A sequence of the droplet evolution from the radial configuration of the director, with a central hedgehog defect, to an axial texture with an equatorial ring defect is shown in the Figure 2.

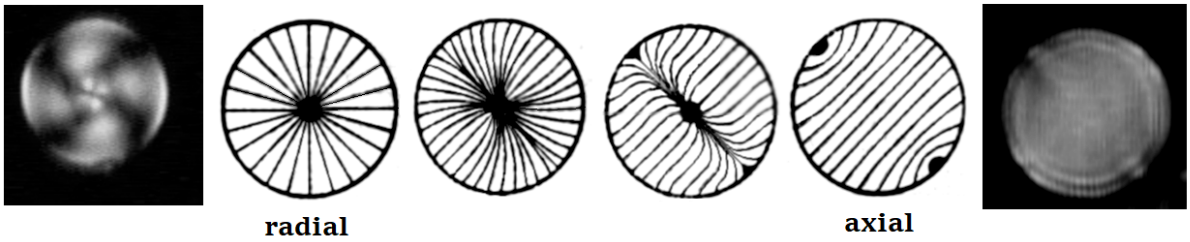

Figure 2 - Direction of the nematic director for a spherical droplet in an electric field: from left to right, radial structure, $E=0$; appearance and compression of domain wall in the equatorial plane, $E>0$; axial structure for $E>E_{th}$, that is, above a threshold value. On the left and on the right, two droplets observed by means of the polarized light microscope with crossed polarisers.

Kralj and Zumer [16] discussed droplets with homeotropic anchoring by means of a numerical solution of Euler-Lagrange equation from the elastic theory. Other numerical approaches elaborate descriptions of the PDLC film behaviour [17-22].

4. Radial and axial configurations

In this section we will see how simply evaluating the threshold field for a radial droplet. First of all, it must be observed that the field in the droplet E_{in} is different from the applied external field [23]. An accepted evaluation of E_{in} is the following [24]:

$$E_{in}=\frac{3U\varepsilon_P}{d\left(2\varepsilon_P+\varepsilon_{LC}\right)} \qquad (1)$$

In (1), U is the applied voltage to PDLC film, d is the film thickness, ε_{LC} , ε_P the average dielectric constants of the liquid crystals and the polymer. This equation is valid for the complex dielectric constant too, then also for slightly conducting liquid crystals.
Let us start from the elastic free energy density in one elastic constant approximation [25]:

$$f_{el}=\frac{k}{2}\left[(\nabla\cdot\boldsymbol{n})^2+(\nabla\times\boldsymbol{n})^2\right] \qquad (2)$$

In (2), k is the elastic constant and $\boldsymbol{n}$ the director field. Let us consider a frame of reference as given in the Figure 3.

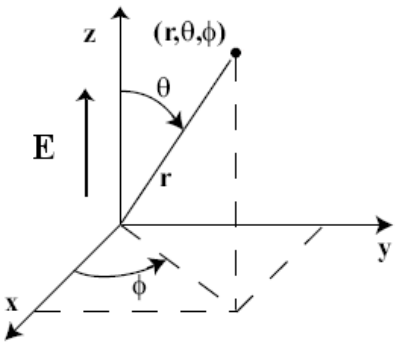

Figure 3 – Frame of reference for calculations.

In the case of a droplet in the radial configuration, the nematic director is given by: $\boldsymbol{n}=(x/r)\boldsymbol{i}+(y/r)\boldsymbol{j}+(z/r)\boldsymbol{k}$. Its divergence is $div\,\boldsymbol{n}=2/r$, whereas its rotor is null. The elastic free-energy density is therefore : $f_{el}=(k/2)\cdot(2/r)^2$. In the case of a spherical droplet with radius *R*, the total elastic energy in the bulk for a radial texture is given by:

$$F_{el}=\frac{k}{2}\iiint (div\ \boldsymbol{n})^2 r^2 dr\ \sin\theta\ d\theta\ d\varphi=2k\iiint dr\ \sin\theta\ d\theta\ d\varphi=8\pi kR \quad (3)$$

Considering $\boldsymbol{n}_o$ the easy unit vector at the surface, let us suppose a surface energy of the form:

$$F_{surf}=-\frac{1}{2}WR^2\iint (\boldsymbol{n}\cdot\boldsymbol{n}_o)^2\sin\theta\ d\theta\ d\varphi \qquad (4)$$

W has the dimension of an energy divided by the square of a length. The surface energy has its minimum value in the radial configuration, if the anchoring conditions are favoring the molecules as perpendicular to the surface ($\boldsymbol{n}_o$ perpendicular to the surface) [26]. The surface energy can be written also in other forms [27,28], which are equivalent to the Rapini-Papoular form (4).
In the case of a strong anchoring:

$$F_{surf}=-2\pi WR^2$$

When an electric field $\boldsymbol{E}=E\boldsymbol{k}$ is applied parallel to a given *z*-axis, a further contribution to the free energy density in the form $-\varepsilon_a\varepsilon_o(\boldsymbol{E}\cdot\boldsymbol{n})^2/2$ must be considered [25]. In the given framework: $(\boldsymbol{E}\cdot\boldsymbol{n})^2=E^2\cos^2\theta$. Therefore, on the volume of the droplet:

$$F_{radial}=-2\pi WR^2+8\pi kR-\frac{\varepsilon_a\varepsilon_o E^2}{2}\iiint \cos^2\theta\cdot r^2 dr\ \sin\theta\ d\theta\ d\varphi$$

$$F_{radial}=-2\pi WR^2+8\pi kR-\varepsilon_a\varepsilon_o 2\pi E^2R^3/9 \quad (5)$$

where ε_a is the relative anisotropic dielectric constant. To compare F_{radial} with the free energy in axial configuration, let us assume in this configuration the director parallel to *z*-axis. The presence of an equatorial ring defect is not considered. The director is then $\boldsymbol{n}=\boldsymbol{k}$, and no elastic deformation exists. However, we have a surface contribution too. Then:

$$F_{axial}=-\frac{R^2W}{2}\iint\cos^2\theta\ \sin\theta d\theta\ d\varphi-\frac{\varepsilon_a\varepsilon_o E^2}{2}\iiint r^2 dr\ \sin\theta d\theta\ d\varphi=-\frac{2\pi R^2W}{3}-\frac{\varepsilon_a\varepsilon_o 2\pi E^2R^3}{3}$$

(6)

where W is the anchoring strength, with the conventional Rapini-Papoular form of surface anchoring free energy density.
The stable texture is that having the lower free energy. Comparing F_{radial} and F_{axial}, we could find the threshold value E_{th}, so that, for greater values of the field the axial structure is favoured. Let us remember the two expressions (5) and (6):

$$F_{radial}=-2\pi WR^2+8\pi kR-\varepsilon_a\varepsilon_o 2\pi E^2R^3/9 \;\; ; \;\; F_{axial}=-\frac{2\pi R^2W}{3}-\frac{\varepsilon_a\epsilon_o 2\pi E^2R^3}{3}$$

Comparing free energies, the threshold field as a function of the droplet radius can be obtained:

$$\frac{4\varepsilon_a\epsilon_o E^2}{9}=\frac{4W}{3R}-\frac{8k}{R^2} \quad (7)$$

To have a solution, we need W greater than $6k$/R. k is assumed 10^{-6} cgs.
Experimental data from Ref. [13] are given in Fig.4. The electric field threshold is decreasing with the increase of the droplet diameter d.

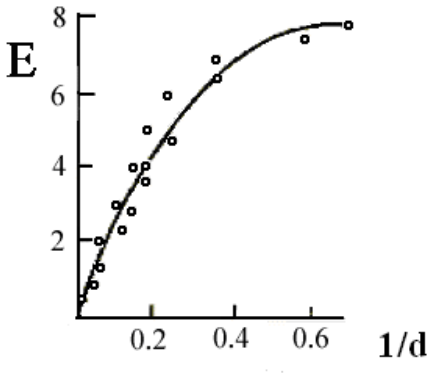

Figure 4: Threshold external field E vs the reciprocal of the droplet diameter under normal boundary condition. E is in $10^6 V/m$, $1/d$ *in* $10^6 m^{-1}$. Data as given in [13].

Let us evaluate the threshold from (7). Let us assume $W\sim10^{-1}$ cgs, $k\sim10^{-6}$ cgs and $R\sim10^{-3}cm$.

$$\frac{4\varepsilon_a\varepsilon_o E^2}{9}=\left(\frac{4\times10^{-1}}{3\times10^{-3}}-\frac{8\times10^{-6}}{10^{-6}}\right)\frac{dyn}{cm^2}=\left(1.3\times10^2-8\right)\frac{dyn}{cm^2}\sim120\frac{dyn}{cm^2}$$

So we have, assuming $\varepsilon_a=2$:

$$E^2\sim120\frac{dyn}{cm^2}\times\frac{9}{4}\times(\varepsilon_o)^{-1}=120\frac{dyn}{cm^2}\times\frac{9}{4}\times\frac{10^{21}}{8.85}\frac{dyn\cdot cm^2}{C^2}=305\times10^{20}\frac{dyn^2}{C^2}$$

Therefore, the value of the electric field to drive the transition is of about:

$$E \sim \sqrt{305} \times 10^{10} \frac{dyn}{C} = 17.5 \times 10^{5} \frac{N}{C} = 1.75 \times 10^{6} \frac{V}{m}$$

And this result is in agreement to the value that we can find given in the Figure 4 (actually $2. \times 10^{6} V/m$). We could also consider the shape of the droplets and its influence in determining the threshold of the electric field, required to switch the film between opaque and transparent state. We do not discuss it, because it is behind the aim of the article.

5. Bipolar droplets

When the surface between the liquid crystal and the polymer is favoring a locally planar configuration at the surface of the droplet, the nematic inside the droplet assumes a bipolar texture [29]. Let us suppose that the electrical field is zero. The bipolar droplet axes have a random configuration as in the Fig.5, where the axis direction of each droplet is fixed by its surface. When the electric field is turned on and increases above a threshold value, droplets become all oriented parallel to the field.

Here we will consider spherical droplets. In fact, we could also consider different shapes of the droplets and determine the threshold value of the electric field, required to switch the film from the opaque to the transparent state, but this is beyond the aim of this discussion.

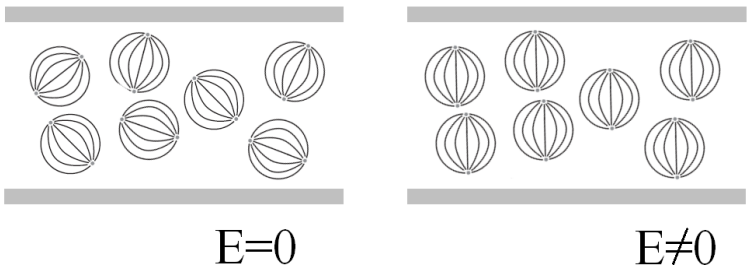

Figure 5. Bipolar droplets without and with an electrical field applied to the film: if *E=0*, bipolar droplet axes assume a random configuration but when the electric field is above a threshold value, droplets are all oriented parallel to the field.

Just to understand, in a rough manner, the competing role of orientation of the droplets and electric field, let us use the following approach.
Let us describe the droplet bipolar axis by means of a dimensionless unit vector $\boldsymbol{L}$. Each droplet possesses a preferred direction $\boldsymbol{L}_o$: it is the direction assumed by the bipolar axis when no field is present. The interaction between the easy axis, described by a dimensionless unit vector $\boldsymbol{L}_o$, and the actual droplet axis $\boldsymbol{L}$ can be assumed as:

$$f_{in} = -w(\boldsymbol{L}\cdot\boldsymbol{L_o})^2 \quad (12)$$

in the unit volume. In the configuration with the droplets oriented along the easy directions, the free energy is $f_{in} = -n\,w$, with n number of droplets in the unit volume.
To evaluate the free energy contribution coming from the presence of the electric field, let us consider the distribution of the axis direction $\boldsymbol{L_o}$, with respect to the axis of the electric field $\boldsymbol{E}$, as a uniform distribution. In fact, we are assuming that the droplets have a random distribution of axes, and this is reasonable in the case of spherical droplets. Averaging on the angle θ, that is the angle between $\boldsymbol{E}$ and $\boldsymbol{L_o}$ (see Figure 3), the contribution to the free energy coming from the interaction between droplets and field is:

$$f_{diel} = -\frac{\varepsilon_a \varepsilon_o n}{2\pi}\int_0^{\pi}\left(\boldsymbol{E}\cdot\boldsymbol{L_o}\right)^2 d\theta \quad = -\frac{\varepsilon_a \varepsilon_o n E^2}{4} \quad (13)$$

The total free energy is:

$$f_{disord} = f_{in} + f_{diel} = -n\,w - \frac{\varepsilon_a \varepsilon_o n E^2}{4} \quad (14)$$

In the case that we consider a configuration with the axes of droplets aligned with the external field, a contribution to the total free energy is coming from the interaction of the actual droplet axis direction $\boldsymbol{L}$ with the easy axis direction $\boldsymbol{L_o}$, and then the free energy can be estimated as the following average:

$$f_{in} = -\frac{nw}{\pi}\int_0^{\pi}(\boldsymbol{L}\cdot\boldsymbol{L_o})^2 d\theta = -\frac{nw}{2} \quad (15)$$

We have also the contribution coming from the presence of external electric field to the free energy. In this case:

$$f_{elet} = -\varepsilon_a \varepsilon_o n(\boldsymbol{L}\cdot\boldsymbol{E})^2/2 = -\frac{\varepsilon_a \varepsilon_o n}{2}E^2 \quad (16)$$

since $\boldsymbol{L}$ and $\boldsymbol{E}$ are parallel. The total free energy is:

$$f_{unif} = f_{in} + f_{elet} = -\frac{nw}{2} - \frac{\varepsilon_a \varepsilon_o n}{2}E^2 \quad (17)$$

Comparing the free energy in the case of a uniform axes distribution with that obtained with a disordered configuration (14), we can see the existence of a threshold field E_{th} above which the stable configuration is the uniform one. Imposing $F_{disord} = F_{unif}$, the threshold field is:

$$\frac{\varepsilon_a \varepsilon_o}{2}E^2 = w \quad (18)$$

To know the value of the field, an independent estimate of the parameter *w* is necessary.

The discussion given above is just a simple approach to show the existence of a threshold value for the electric field. For a rigorous approach to the reorientation of LC droplets by an electric field, it is necessary to consider the droplet dynamics in terms of electric, elastic and viscous torques. The elastic-restoring torque per unit volume depends on the variation in the elastic free-energy density of the droplet with some orientational parameter for the droplet. The viscous torque can be represented also with a rate of reorientation and a rotation viscosity coefficient. The electric torque per unit volume depends on the electric field free energy density. Rise and decay times are determined by balancing all the torques [30-32].

As previously told, the approach that we followed is like that proposed in [33]. The aim was just that of showing the existance of a threshold value for the electric field.

6. Methods of PDLC preparation

The formation of uniform liquid crystal droplets in a polymer binder may be achieved by several different phase separation processes which include phase separations by polymerization, thermal processes, and solvent evaporation. Each approach involves preparing a homogeneous solution of monomer or prepolymer with a liquid crystal material followed by phase separation, droplet formation, and finally, polymer solidification or gelation. These processes are a result of droplet nucleation and growth.

Phase separation methods are simply one-step processes which can reduce fabrication costs in display and window applications. Phase separation by polymerization (PIPS) is useful when prepolymer materials are miscible with low molecular weight liquid crystal compounds [34]. A homogeneous solution is made by mixing the prepolymer with the liquid crystal. Polymerization is achieved through a condensation reaction or with a free-radical polymerization, catalyzed by a free-radical initiator, or through a photoinitiated polymerization.

The solubility of the liquid crystal decreases in the stiffening polymer until the liquid crystal phase separates, forming droplets. The droplets grow until polymer stops the change of droplet morphology. Droplet size and morphology are then determined during the time between droplet nucleation and gelation of the polymer. The size is controlled by the rate of polymerization, relative concentrations of materials, types of liquid crystal and polymers used, and by such physical parameters as viscosity, rate of diffusion, and solubility of the liquid crystal in the polymer. The rate of polymerization is controlled by the temperature for thermally cured polymers or by light intensity for photochemical polymerization.

Phase separation by thermal processes is useful for thermoplastics which melt below their decomposition temperature. A binary mixture of polymer and liquid crystal forms a homogeneous solution at high temperature. Cooling the homogeneous solution causes phase separation of the liquid crystal: the droplet size of the liquid crystal is governed by the rate of cooling and depends upon material parameters, which include viscosity, chemical potentials, and so on. Some polymers, for instance polymethyl-methacrylate (PMMA), form droplet dispersions with cyanobiphenyl liquid crystal materials [35,36].

Phase separation by solvent evaporation is useful with thermoplastics which melt above the decomposition temperature of the thermoplastic or the liquid crystal, or where solvent coating

techniques are used. Liquid crystal and polymer are dissolved in a common solvent forming a homogeneous solution. Then, solvent is removed by evaporation, resulting in phase separation and polymer solidification. Further processing, such as laminating a cover substrate, is performed, followed by a final annealing step where film is warmed to redissolve the liquid crystal in the polymer and cooled at a rate chosen to give the desired droplet shape and density. The solvent evaporation process followed by thermal annealing adds flexibility and makes easier the production of commercial PDLC films.

7. Several blends of materials

The relationships between the structure and the electro-optical properties of PDLCs have been examined extensively. Of course, the properties of the liquid crystalline materials such as elastic constants, viscosity, dielectric anisotropy or birefringence, and electro-optical responses are important; however, even more important are the properties that they acquire inside the polymer of PDLC films. These properties are strongly dependent on the polymer structure and thus, on the nature of the blend and of the rate of polymerization mechanisms. Consequently, several blends of materials have been prepared and studied to have specific responses. Here let us discuss some of the resulting materials.

Liquid crystals, polymers and dyes have been studied to have color PDLC films, by incorporating dyes of isotropic or dichroic type in the films. In [37], it was explained that colored PDLC shutters are formed by the inclusion of isotropic dyes in the epoxy resin and liquid crystal. After PDLC is formed, the dye is dissolved in both the epoxy binder and the liquid crystal droplets The shutters are highly colored and are scattering in the absence of an aligning electric field. In the scattering state, that is in the OFF state, the path length of light is increased due to Rayleigh-Gans and multiple scattering. Actually, the color contrast of the PDLC film incorporating an isotropic dye is resulting from path-length change of light passing through the film, in the scattering and transparent states. The scattering efficiency of the PDLC film depends on the absorbance of the isotropic dye [38,39].

In the case that dichroic dyes are dissolved in the liquid crystal droplets, we have higher color contrast than in the case that the isotropic dyes are used. Dichroic dyes are aligned by the liquid crystal in the droplets and therefore its absorption is modulated by alignment of mesogen with an electric field. In one state OFF, the alignment of dichroic dyes varies randomly from droplet to droplet. In the other state ON, droplet directors and dichroic dyes are aligned normal to the film surface. Let us note that, dichroic dye dissolved in the polymer binder will be randomly aligned and unaffected by an applied electric field. Only the dye dissolved in the droplet will exhibit its dichroic properties and improve the contrast of the PDLC display compared to the use of isotropic dyes. The segregation of dye in LC droplets was found to be dependent on the type of dye by West [40].

In [41], the blend which is used is incorporating a dichroic azo dye Disperse red 1. The PDLC is obtained by polymerization induced phase separation (PIPS) method. The research shows that the phase separation and the segregation of LC droplets is dependent on the amount of dye used. Moreover, PDLC with low dye content (≤0.06 wt%) gave a good contrast ratio, relatively low threshold voltage and a value of high transmittance in the ON-state. As noted in [41], the use of PDLC devices is restricted by the low contrast ratio and high threshold field; the use of a dichroic dye can enhance the electro-optical performance of the film.

Other studies on blends with dichroic dye, that is on D-PDLCs, are given in [42-47].

The films obtained from blends containing dyes are also known as Guest-Host (G-H) Polymer Dispersed Liquid Crystal (PDLC) films. "Guest" in this case is a dye, "Host" is a type of liquid crystal. A dichroic dye is used. As told before, the "guest" dye molecules are oriented in the medium by the bistable host liquid crystal molecules to display and retain images. In [48], to create the GH-PDLC layers, droplets of Smectic A liquid crystal mixed with dichroic dye were dispersed in a polymer binder. The films were used to have a rewritable medium. The medium was thermally written and electrically erased.

Other works on GH-PDLCs and digital papers are given in [49-53]

8. Holographically formed PDLCs

Holographic recording materials based on photopolymerizable systems have contributed to the growth of holographic application. A holographic grating can be made in photopolymer films via a single-step process at a relatively fast speed. The possibility of applying electrically and optically switchable holographic grating gained increasing interest at the end of the past century [54-56], so that several researches had been made subsequently on H-PDLCs, that is, on the holographically formed PDLCs. In any case, H-PDLCs are a variant of the conventional PDLCs, formed under holographic conditions [57,58].

H-PDLCs films are made of polymers and liquid crystals that have been treated by a laser beam to form a reflective Bragg grating. In the films, a spatial variation of light intensity is giving a patterned LC droplet distribution. The spatially varying differences of the two-phase structures that we can obtain, are very important in determining the performance of the related switchable diffractive structures, which can be transmissive or reflective.

In the blend of a liquid crystal and a photo-sensitive monomer, by interfering laser beams it is produced a standing wave pattern. The two main constituents of the blend form a film where we have a separation into polymer rich layers and liquid crystal rich layers. Instead of random arrays of droplets like in the conventional PDLC technology, the holography introduces a periodic array of liquid crystal droplets and solid polymer planes. The interference fringe spacing, L, of the grating is described by:

$$L = \lambda / (2n\,|\sin(\alpha)|) \qquad (19)$$

where λ is the wavelength of the exposing laser, n is the average index of the material prior to polymerization, and α is half the angle between the exposing beams. If the relative optical indices of the polymer and liquid crystal materials are carefully chosen, the result is a set of planes that reflects light of a specific set of wavelengths and transmits all others. The refractive index difference and the spacing between the layers determine this behavior.

The first application of H-PDLC materials was in the area of reflective display technology. These displays are bright (Bragg reflection >70%), fast switching, yield bright colors and do not suffer from polarizer losses.

When an electric field is applied across the multi-layer H-PDLC film, the liquid crystal material reorients and eliminates the index difference and film becomes transparent to all wavelengths. This capability enabled the H-PDLC technology to be easily integrated to create a full color display, so that a very bright reflection at each pixel was achieved. Actually, the colors were integrated under one electrode structure (see Fig.6), so that color was obtained by

means of a spatial synthesis with pixel that consists of a red, green and blue sub-pixel. In this case, the color is intrinsecally given by the PDLC film and no color filter is used.

One of the primary problems encountered with H-PDLC technology for reflective display applications was that it had a very narrow viewing volume. Although the reflection from H-PDLC pixels was very bright, with excellent color purity and 100 μs switching time, the viewing-angle was specular and narrow (~2°). This reflective display was nearly unusable in any practical setting, but by placing a diffuse film in one of the two interfering laser beams used in formation, a diffuse hologram could have been recorded, having a significantly enhanced viewing cone (~30° wide was possible). This was the method that had been proposed for the practical implementation in [59,60].

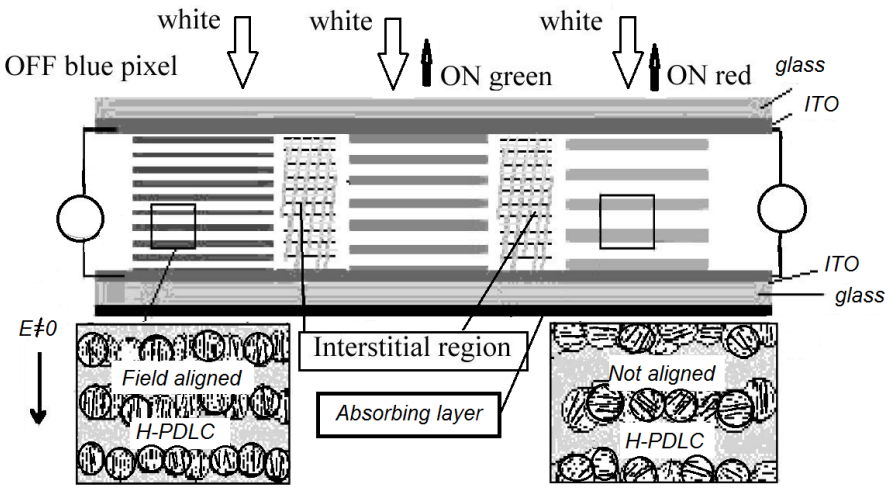

Figure 6: Pixels with different colors in H-PDLC devices. No color filters are used. The drive voltages are reduced to values below 100 volts.

The multiplexing, including angular multiplexing, spatial multiplexing, and temporal multiplexing is commonly used in H-PDLC films. The reason is simple: everything that we can do with conventional holographic processes, can also be performed with switchable holograms. As we have seen, the spatial multiplexing technique allows for the formation of multiple color regions on a single sample. In the angular multiplexing technique, three beams are simultaneously incident on the sample, resulting in the formation of two different reflection gratings and a transmission grating. This can be extended to higher numbers of beams which allows for the creation of additional gratings, such as those investigated in [61]. Multiple gratings can be created at the same specular angle, or at different ones depending on the application. Recent studies on multiplexing H-PDLCs are given in [62-64].

There are a number of other applications for which H-PDLCs can be used. H-PDLC thin films can make switchable microlens arrays, Fresnel lenses, blazed gratings, and others. For example, lens array with a short pitch was fabricated: without an electric field, the converging microlens array reflects at visible wavelengths with a certain focal length, but when an electric field is applied, it becomes transparent (non-reflecting) [65].

9. Polymer Shrinkage

In H-PDLC films it is necessary to consider the effect of polymer shrinkage. The conversion of the monomer molecules into a polymer network is accompanied with closer packing of the molecules, which leads to the bulk contraction denoted as "polymerization shrinkage". Polymerization shrinkage can severely compromise the utility and the performance of the device. For example, in the applications which need to be polarization insensitive, the polymer shrinkage can cause the following problem. When the polymer shrinks, the liquid crystal droplets are compressed; the result is a preferentially alignment of the axes of the droplets along a common direction. This alignment causes a polarization sensitive reflection, since the optical axis is, on average, along the same direction for all droplets. The consequent reflection and diffraction efficiency becomes extremely sensitive to the input polarization.

Monomers commonly used in the preparation of H-PDLCs undergo shrinkage upon polymerization, but the spectroscopy of H-PDLC gratings allows to measure optically and quantify the volumetric changes of photocurable materials during the formation of gratings.

As stressed in [66], "prior to obtaining a wide commercialization of displays based on photopolymers, one of the key aspects is to achieve a complete characterization of them. In this sense, one of the main parameters to estimate and control is the shrinkage of these materials. ... One criteria for the recording material to be used in a holographic data storage application is the shrinkage, maximum of 0.5%".

The used monomers are therefore quite important. The acrylate monomers are known to shrink as much as 10% during polymerization, wheras epoxy based monomers are known to have low shrinkage. Partially fluorinated acrylate monomers are also suitable for preparing H-PDLC films. The presence of fluorine in the polymer chain leads to the strong electrostatic repulsion between the chains thus minimizing the shrinkage during polymerization. Fluorinated monomers may lower the liquid crystal anchoring strength thus lowering the switching voltage in H-PDLC films [67]. In any case, compensation methods, based on a corrected condition in the geometry of optical setup for recording volume holograms, had been proposed to physically correct the shrinkage effect of monomers as soon as H-PDLC films had been developed for optical devices [68].

10. Strain Gauge Applications

An application for the H-PDLC films is for reflecting strain gauges [69]. The peak reflected wavelength depends on the spacing between polymer rich planes and on the refractive index modulation through the depth of the cell (Fig. 7). The optical strain characteristics of a reflective holographic- polymer dispersed liquid crystal (H-PDLC) change with increasing strain. A spectral blue-shift was observed to occur with increasing strain: the spectral dependence on strain is due to Poisson contraction of the material. In addition to the blue-shift, the contraction also preferentially aligned the liquid crystal droplets in the tensile plane, creating highly aligned bipolar droplets. In this state, the reflection becomes highly polarization dependent.

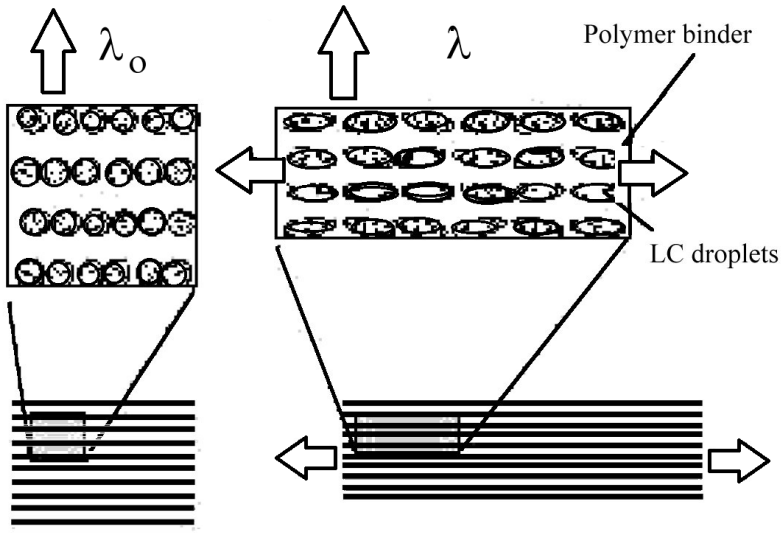

Figure 7: Peak reflected wavelength depends on spacing between planes.

Conclusions

In this paper we have discussed PDLC systems. The threshold electric field is obtained in a medium containing a volume fraction of spherical identical droplets filled with liquid crystal. Droplet boundary conditions which can be either radial or bipolar are adopted. The dependence on the droplet diameter of the threshold field is evaluated for radial texture. For the bipolar droplets, the effect is much more subtle, since it is necessary to have a good evaluation of anchoring strengths.

The paper discussed also some devices obtained with dye doping the droplets or with holographic techniques. When I discussed in 2003 [33] the PDLCs, the research field was in strong development. From that period, the research applied to new technologies had produces, besides a large number of publications, also several new devices. An example: the "digital papers", that in 2003 were prototypes, are today commonly available and used. Therefore, the proposed discussion has to be seen as a picture of the base applications, on which the commercial devices, today available, have been developed.

References

1. Sparavigna, A. C. (2016). James Fergason and His Role in the Basic and Applied Science of Liquid Crystals. Available at SSRN 2859527.
2. Sparavigna, A. C. (2013). James Fergason, a pioneer in advancing of liquid crystal technology. arXiv preprint arXiv:1310.7569.
3. Fergason, J. L. (1981). Encapsulated Liquid Crystal and Method, Issued on March 6, 1984. Application No. 06/302780 filed on 09/16/1981. Patent No. 4435047.

4. Fergason, J. L. (1985). Polymer Encapsulated Nematic Liquid Crystals for Display and Light Control Applications, SID Int. Symp. Dig. Technol., 16, 68–70.
5. Doane, J. W., Vaz, N. A., Wu, B. G., & Zumer, S. (1986). Field Controlled Light Scattering from Nematic Microdroplets, Appl. Phys. Lett., 48(4), 269-271.
6. J.W. Doane, Liquid Crystals-Application and Uses, Vol. 1, World Scientific, Singapore, 1990.
7. P.S. Drzaic, Liquid Crystals Dispersions, World Scientific, Singapore, 1995.
8. V.G. Nazarenko, Yu.A. Reznikov, V.Yu. Reshetnyak, V.V. Sergan, & V.Ya. Zyryanov, (1993). Oriented dispersion of liquid crystal droplets in a polymer matrix with light induced anisotropy. Molecular Materials, 2(4), 295-299.
9. Crawford, G. P., & Zumer, S. (1996). Liquid Crystals in Complex Geometry, Taylor and Francis, London.
10. Dick, V. P., & Loiko, V. A. (2001). Model for coherent transmittance calculation for polymer dispersed liquid crystal films. Liquid Crystals, 28(8), 1193-1198.
11. Amundson, K., Van Blaaderen, A., & Wiltzius, P. (1997). Morphology and electro-optic properties of polymer-dispersed liquid-crystal films. Physical Review E, 55(2), 1646.
12. Amundson, K. (1996). Electro-optic properties of a polymer-dispersed liquid-crystal film: Temperature dependence and phase behavior. Physical Review E, 53(3), 2412-2422.
13. Koval'chuk, A.V., Kurik, M.V., Lavrentovich, O.D., & Sergan, V.V. (1998). Structural transformations in nematic droplets located in an external magnetic field. Sov. Phys. JETP, 67 (5), 1065 (1988).
14. Koval'chuk, A. V., Kurik, M. V., Lavrentovich, O. D., & Sfrgan, V. V. (1990). Electrooptical effects in the polymer dispersed nematic liquid crystals: response times. Molecular Crystals and Liquid Crystals, 193(1), 217-221.
15. Lavrentovich, O.D., & Sergan, V.V. (1990). Parity-breaking phase transition in atangentially anchored nematic droplets. Nuovo Chim. D: Cond. Matter, 12 (9), 1219-1222.
16. Kralj, S., & Žumer, S. (1992). Fréedericksz transitions in supra-μm nematic droplets. Physical Review A, 45(4), 2461.
17. Chiccoli, C., Pasini, P., Skačej, G., Zannoni, C., & Žumer, S. (2000). Dynamical and field effects in polymer-dispersed liquid crystals: Monte Carlo simulations of NMR spectra. Physical Review E, 62(3), 3766-3774.
18. Kyu, T., Nwabunma, D., & Chiu, H. W. (2001). Theoretical simulation of holographic polymer-dispersed liquid-crystal films via pattern photopolymerization-induced phase separation. Physical Review E, 63(6), 061802.
19. Chiccoli, C., Pasini, P., Skačej, G., Zannoni, C., & Žumer, S. (1999). NMR spectra from Monte Carlo simulations of polymer dispersed liquid crystals. Physical Review E, 60(4), 4219-4225.
20. Kelly, J. R., & Palffy-Muhoray, P. (1997). Normal modes of director fluctuations in a nematic droplet. Physical Review E, 55(4), 4378-4381.
21. Teixeira, P. I. C., & Mulder, B. M. (1996). Cell dynamics model of droplet formation in polymer-dispersed liquid crystals. Physical Review E, 53(2), 1805-1815.
22. Berggren, E., Zannoni, C., Chiccoli, C., Pasini, P., & Semeria, F. (1994). Computer simulations of nematic droplets with bipolar boundary conditions. Physical Review E, 50(4), 2929-2939.
23. Berggren, E., Zannoni, C., Chiccoli, C., Pasini, P., & Semeria, F. (1994). Monte Carlo study of the effect of an applied field on the molecular organization of polymer-dispersed liquid-crystal droplets. Physical Review E, 49(1), 614-622.

24. Reshetnyak, V. Y., Sluckin, T. J., & Cox, S. J. (1996). Effective-medium theory of polymer dispersed liquid crystal droplet systems: I. Spherical droplets. Journal of Physics D: Applied Physics, 29(9), 2459-2465.
25. De Gennes, P.G., & Prost, J. (1993). The Physics of Liquid Crystals, Oxford : Clarendon Press.
26. Rapini, A., & Papoular, M. (1969). Distorsion d'une lamelle nématique sous champ magnétique conditions d'ancrage aux parois. Le Journal de Physique Colloques, 30(C4), C4-54.
27. Sparavigna, A., Lavrentovich, O. D., & Strigazzi, A. (1994). Periodic stripe domains and hybrid-alignment regime in nematic liquid crystals: Threshold analysis. Physical Review E, 49(2), 1344.
28. Sparavigna, A., Komitov, L., Lavrentovich, O. D., & Strigazzi, A. (1992). Saddle-splay and periodic instability in a hybrid aligned nematic layer subjected to a normal magnetic field. Journal de Physique II, 2(10), 1881-1888.
29. Cox, S. J., Reshetnyak, V. Y., & Sluckin, T. J. (1998). Effective medium theory of light scattering in polymer dispersed liquid crystal films. Journal of Physics D: Applied Physics, 31(14), 1611.
30. Roussel, F., Canlet, C., & Fung, B. M. (2002). Morphology and orientational order of nematic liquid crystal droplets confined in a polymer matrix. Physical Review E, 65(2), 021701.
31. Sharma, S. C., Zhang, L., Tapiawala, A. J., & Jain, P. C. (2001). Evidence for droplet reorientation and interfacial charges in a polymer-dispersed liquid-crystal cell. Physical review letters, 87(10), 105501.
32. Čopič, M., & Mertelj, A. (1998). Reorientation in random potential: A model for glasslike dynamics in confined liquid crystals. Physical review letters, 80(7), 1449.
33. Sparavigna, A. C. (2003). New performances from the electro-optical devices with PDLC-films. Recent Res. Devel. Applied Phys. 6(2003), 797-811.
34. Lee, J. C. (1999). Polymerization-induced phase separation. Physical Review E, 60(2), 1930.
35. Doane, J. W. (1991). Polymer-dispersed liquid crystals: Boojums at work. MRS Bulletin, 16(1), 22-28.
36. Mucha, M. (2003). Polymer as an important component of blends and composites with liquid crystals. Progress in polymer science, 28(5), 837-873.
37. West, J. L., Tamura-Lis, W., & Ondris, R. (1989, July). Polymer dispersed liquid crystals incorporating isotropic dyes. In Liquid Crystal Chemistry, Physics, and Applications (Vol. 1080, pp. 48-52). International Society for Optics and Photonics.
38. Francescangeli, O., Slussarenko, S., Simoni, F., Andrienko, D., Reshetnyak, V., & Reznikov, Y. (1999). Light-induced surface sliding of the nematic director in liquid crystals. Physical review letters, 82(9), 1855.
39. Lucchetti, L., Simoni, F., & Reznikov, Y. (1999). Fast optical recording in dye-doped liquid crystals. Optics letters, 24(15), 1062-1064.
40. West, J. L. (1988). Phase separation of liquid crystals in polymers. Molecular Crystals and Liquid Crystals Incorporating Nonlinear Optics, 157(1), 427-441.
41. Deshmukh, R. R., & Malik, M. K. (2013). Effect of dichroic dye on phase separation kinetics and electro-optical characteristics of polymer dispersed liquid crystals. Journal of Physics and Chemistry of Solids, 74(2), 215-224.
42. Kumar, P., & Raina, K. K. (2007). Morphological and electro-optical responses of dichroic polymer dispersed liquid crystal films. Current Applied Physics, 7(6), 636-642.

43. West, J. L., Ondris-Crawford, R., & Erdmann, M. A. (1990, April). Dichroic dye containing polymer-dispersed liquid crystal films. In Liquid Crystal Displays and Applications (Vol. 1257, pp. 76-83). International Society for Optics and Photonics.
44. Yu, B. H., Huh, J. W., Kim, K. H., & Yoon, T. H. (2013). Light shutter using dichroic-dye-doped long-pitch cholesteric liquid crystals. Optics express, 21(24), 29332-29337.
45. Kumar, P., Kang, S. W., Lee, S. H., & Raina, K. K. (2011). Analysis of dichroic dye-doped polymer-dispersed liquid crystal materials for display devices. Thin solid films, 520(1), 457-463.
46. Malik, P., & Raina, K. K. (2010). Dichroic dye-dependent studies in guest–host polymer-dispersed liquid crystal films. Physica B: Condensed Matter, 405(1), 161-166.
47. Ahmad, F., Jamil, M., Jeon, Y. J., Woo, L. J., Jung, J. E., & Jang, J. E. (2012). Investigation of nonionic diazo dye-doped polymer dispersed liquid crystal film. Bulletin of Materials Science, 35(2), 221-231.
48. Sekine, K., & Saito, W. (2002). PDLC rewritable medium. IEICE transactions on electronics, 85(5), 1151-1155.
49. Fuh, A. Y. G., Tsai, M. S., Huang, L. J., & Liu, T. C. (1999). Optically switchable gratings based on polymer-dispersed liquid crystal films doped with a guest–host dye. Applied physics letters, 74(18), 2572-2574.
50. Malik, P., & Raina, K. K. (2010). Dichroic dye-dependent studies in guest–host polymer-dispersed liquid crystal films. Physica B: Condensed Matter, 405(1), 161-166.
51. Fuh, A. Y. G., Tsai, M. S., Lee, C. R., & Fan, Y. H. (2000). Dynamical studies of gratings formed in polymer-dispersed liquid crystal films doped with a guest-host dye. Physical Review E, 62(3), 3702.
52. Jung, J. E., Lee, G. H., Jang, J. E., Hwang, K. Y., Ahmad, F., Muhammad, J., Woo Lee, J. & Jeon, Y. J. (2011). Optical enhancement of dye-doped PDLC by additional dye-LC layer coating. Optical Materials, 34(1), 256-260.
53. Yoshikawa, H., Omodani, M., Nakamura, K., & Takahashi, Y. (2003). Digital Paper with guest-host type liquid crystal medium. Journal of Imaging Science and Technology, 47(4), 304-308.
54. Holmes, M. E., & Malcuit, M. S. (2002). Controlling the anisotropy of holographic polymer-dispersed liquid-crystal gratings. Physical Review E, 65(6), 066603.
55. Fuh, A. Y. G., Tsai, M. S., Lee, C. R., & Fan, Y. H. (2000). Dynamical studies of gratings formed in polymer-dispersed liquid crystal films doped with a guest-host dye. Physical Review E, 62(3), 3702.
56. Vicari, L. (1998). Reorientation gratings in polymer dispersed liquid crystals. Physical Review E, 58(3), 3280.
57. Bowley, C. C., Crawford, G. P., & Yuan, H. (1999). Reflection from dual-domains in a holographically-formed polymer-dispersed liquid crystal material. Applied physics letters, 74(21), 3096-3098.
58. Bowley, C. C., Fontecchio, A. K., Crawford, G. P., Lin, J. J., Li, L., & Faris, S. (2000). Multiple gratings simultaneously formed in holographic polymer-dispersed liquid-crystal displays. Applied Physics Letters, 76(5), 523-525.
59. Escuti, M. J., Kossyrev, P., Crawford, G. P., Fiske, T. G., Colegrove, J., & Silverstein, L. D. (2000). Expanded viewing-angle reflection from diffuse holographic-polymer dispersed liquid crystal films. Applied Physics Letters, 77(26), 4262-4264.
60. M. J. Escuti, P. Kossyrev, C. C. Bowley, S. Danworaphong, G. P. Crawford, T. G. Fiske, J. Colegrove, L. D. Silverstein, A. Lewis, & H. Yuan (2000, May). P-58: Diffuse H-PDLC Reflective Displays: An Enhanced Viewing-Angle Approach. In SID Symposium

Digest of Technical Papers (Vol. 31, No. 1, pp. 766-769). Oxford, UK: Blackwell Publishing Ltd.
61. Kim, E. H., & Jung, Y. G. (2015). Multiplexing storage using angular variation in a transmission holographic polymer dispersed liquid crystal. Thin Solid Films, 596, 264-268.
62. Fontecchio, Adam K., and Kashma Rai. "Dynamic time multiplexing fabrication of holographic polymer dispersed liquid crystals for increased wavelength sensitivity." U.S. Patent 9,625,878, issued April 18, 2017.
63. Deshmukh, R. R., & Katariya-Jain, A. (2016). Novel techniques of PDLC film preparation furnishing manifold properties in a single device. Liquid Crystals, 43(2), 256-267.
64. Xiao, J., Liu, J., Lv, Z., Shi, X., & Han, J. (2019). On-axis near-eye display system based on directional scattering holographic waveguide and curved goggle. Optics express, 27(2), 1683-1692.
65. Fontecchio, A. K., Escuti, M. J., Bowley, C. C., Sethumadhavan, B., Crawford, G. P., Li, L., & Faris, S. (2000, May). P-60: Spatially Pixelated Reflective Arrays from Holographic-Polymer Dispersed Liquid Crystals. In SID Symposium Digest of Technical Papers (Vol. 31, No. 1, pp. 774-777). Oxford, UK: Blackwell Publishing Ltd.
66. R. Fernández, S. Gallego, A. Márquez, J. Francés, V. Navarro Fuster, C. Neipp, M. Ortuño, A. Beléndez, I. Pascual (2017, May). Shrinkage measurement for holographic recording materials. In Holography: Advances and Modern Trends V (Vol. 10233, p. 102330C). International Society for Optics and Photonics.
67. De Sarkar, M., Qi, J., & Crawford, G. P. (2002). Influence of partial matrix fluorination on morphology and performance of HPDLC transmission gratings. Polymer, 43(26), 7335-7344.
68. Zhao, C., Liu, J., Fu, Z., & Chen, R. T. (1997, April). Shrinkage correction of volume phase holograms for optical interconnects. In Optoelectronic Interconnects and Packaging IV (Vol. 3005, pp. 224-229). International Society for Optics and Photonics.
69. Cairns, D. R., Bowley, C. C., Danworaphong, S., Fontecchio, A. K., Crawford, G. P., Li, L., & Faris, S. M. (2000). Optical strain characteristics of holographically formed polymer-dispersed liquid crystal films. Applied Physics Letters, 77(17), 2677-2679.